RESEARCHERID
THOMSON REUTERS

[Kim, 5(10): October 2018]
DOI- 10.5281/zenodo.1445494

ISSN 2348 – 8034
Impact Factor- 5.070

GLOBAL JOURNAL OF ENGINEERING SCIENCE AND RESEARCHES

CORE SHELL METAL SULFIDE COMPOSITE DECORATED WITH MNO_2ON ZNO NANORODS AS AN EFFICIENT MATERIAL FOR SUPERCAPACITOR

Ikkurthi Kanaka Durga[a], S. Srinivasa Rao[b*], P Himasree[a], T.N.V Krishna[a], S.V.S.V. Prabhu Deva Kumar[a], & Hee-Je Kim[a*]

[a]School of Electrical Engineering, Pusan National University, Gumjeong-Ku, Jangjeong-Dong, Busan 46241, South Korea.

[b]Department of Mechatronics Engineering, Kyungsung University, Busan 46241, South Korea

Abstract

Attention has been paid to the fabrication of Core shell metal sulfide composite materials with MnO_2 on nickel foamfor high-performance supercapacitors. We have prepared unique hetero-structures on nickel foam, which was accomplished through a facile and cost-effective chemical bath deposition method, hydrothermal method, combined with dip coating process and drop casting. Metal sulfides have enticed substantial attention owing to their outstanding properties and used in multiple application areas, such as electrochemical energy conversion and energy storage.Here we describe a cost-effective and facile solution approach for the preparation of metal sulfide (CuS) grown on ZnO NRs as a good electrical conductor and facilitating the polymer shell to grow on them. A maximum specific capacitance of 2554.61 and 2040.73 F g^{-1} are measured for ZnONRs@CuS@PEDOT: PSS@MnO_2 and ZnONRs@CuS@PEDOT: PSS, respectively at 0.71 A g^{-1}, whereas the pure ZnO and ZnO@CuS exhibits a specific capacitance of 24.77 and 1709.34 F g^{-1}. After 3000 cycles at a high current density of 1.2 A g^{-1}, the retention rate is 94%, indicating good long-term cycling stability. These results indicate that the ZnO NRs@CuS@PEDOT:PSS@MnO_2 electrode has large electrode/electrolyte interface, which offers more active sites and ensures a high charge storage capacity, which is a promising for high-performance supercapacitor applications.

Keywords: *Supercapacitors; Copper sulfide; PEDOT:PSS; MnO_2; Core-shell.*

I. INTRODUCTION

Among the transition metal oxides considered to date, zinc oxide (ZnO) is considered to be one of the promising candidates which can be used for supercapacitor applications as a result of its good electrochemical activity, low cost and environmental friendliness [1-2].ZnO and its hybrid structures can be exploited in variety of applications such as solar cells, transparent conducting oxides, gas sensors and photo detectors. Despite the fact that ZnO is an encouraging material, regrettably there is an obstacle of the zinc oxides applicability because of its low rate capability, poor electrical conductivity and cyclic stability in its pure form [3-4].One way to address these concerns is by forming nanocomposites of 1D with other materials. Semiconducting 1D ZnO nanostructures usually have high aspect ratio, high surface area and high crystalline quality that provides a direct conduction path for electrons [5]. The synergetic enhancement in the properties arises in the composite that helps in improving the performance of the material.

Benefits of both the capacitances of the metal oxides and the double layer capacitance in turn improves the capacitance and cyclic stability. Additionally, the core-shell structure not only guarantees stable structure and favorable kinetics but also provides high surface area which increases the amount of active sites on the surface of materials [6]. Comparable to metal oxides, metal sulfides have been established as capable anode materials for supercapacitors (SCs).Recently, numerous metal sulfides such asNiS, MnS, CuS, CoS_2, ZnS and MoS_2 have been investigated as the electrode material of SCs.Metal oxide and metal sulfide based electrode materials are more stimulating towards SC applications owing to its high specific capacitance, enhanced redox reversibility and high

electrical conductivity. The complex hierarchical core-shell nanostructures are considered as a promising approach that can improve the supercapacitor performances [7].

To enhance the electrochemical capacitance of supercapacitors, various types of composite nanomaterials have been used as active electrode materials, such as metal oxide, metal sulfides, and conducting polymers. Among the metal sulfides NiS and CuS have been extensively studied due to their high theoretical specific capacitances and electrical conductivity [8].The electronegativity of sulfur is low when compared to oxygen which makes it easy for electron transport and the replacement of oxygen with sulfur provides flexibility in fabrication of nanomaterials. Copper sulfide (CuS) is one of the most attractive multifunctional energized nanomaterials with many different morphological phases. Chalcocite (Cu_2S), villamaninite (CuS_2), djurleite (Cu1.95S), anilite (Cu1.75S), and covellite (CuS) have been studied extensively for electronics devices, solar cells, gas sensors, and photo-catalysis due to their ease of electric conduction, optoelectronic properties, excellent chemical and thermal stability [9-11].Nickel Sulfide (NiS) has also been widely examined and boundless applications in supercapacitors, lithium ion batteries, dye-sensitized solar cells and ceramic toughеners etc.NiS is the high-performance supercapacitor electrode, which have excellent electrochemical performance due to their unique structure, high surface area and large in-plane conductivity, enhanced structural stability has provoked amusing attention with the advantage of high electronic conduction, ease of fabrication, low cost, and low toxicity [12].Although NiS have excellent electrochemical performance, the drawbacks of these material are their short life cycles when compared with CuS.In the recent past CuS have been extensively used in photo-catalysts, solar cells, lithium-ion batteries and so on due to their higher electronic conductivity (103 S cm^{-1}), a high theoretical capacity (561 mA h g^{-1}), complex structures and valence states [13-14]. Recently, preparations of nanostructures of CuS composites have been verified to show enhanced energy storage properties.

MnO_2 is generally considered to be one of the most encouraging candidates for supercapacitor because of its high theoretical specific capacitance, low cost, environmentally friendliness and abundance in nature [15]. However, the poor electrical conductivity of MnO_2 effects in a low gravimetric capacitance and thus holds back the wide application in energy storage systems [16].Poly (3,4-ethylenedioxythiophene)/poly(strenesulfonate) (PEDOT:PSS) was discovered in the 1980s and it has since been used in many industries because of its optical properties, high conductivity, ease of synthesis and stability in high humidity and high temperature. Moreover, PEDOT:PSS is considered a promising material for SC electrodes because of its excellent chemical and electrochemical stability and ability to be dispersed in various solvents.An effective strategy is to combine MnO_2 with intrinsic conductive polymers e.g. polypyrrole (PPy), poly(3,4-ethylenedioxythiophene) (PEDOT), poly(3,4-ethylenedioxythiophene):poly(styrenesulfonate) (PEDOT:PSS)and polyaniline (PANI).PEDOT:PSS effectively strengthens the electrochemical properties [17]. The outstanding electrochemical performances of the hierarchical films are very difficult to achieve from a single common material. These approaches are slowly becoming more important for producing effective supercapacitors. A myriad of transition oxide/sulfide materials are fabricated on nickel foam (NF) due to its high porosity and highly accessible open structure which guarantees large amounts of active sites for redox reaction and ion diffusion.NF is acted as template for the growth of materials due to its high conductivity with porous structure.

Here, we designed and synthesized hierarchically assembled ZnO nanorods (NRs) with catalytically active metal sulfide (CuS) materials on nickel foam substrate to efficientlyincrease the electron transfer to the NR current collector, facilitating the polymer (PEDOT: PSS) shell to grow on them. The effect of metal sulfide plays a major role in enhancing the capacitance of the fabricated electrode. At last the decoration of the ZnONR@CuS@PEDOT:PSS nanostructures by MnO_2 is done. The techniques employed for the synthesis of this hybrid electrode material have the advantages of low temperature, cost effective and less time consuming compared to those that are based on hard templates. Moreover, the hierarchical structure with high specific area which improves the density of active sites and enhances the density of active sites, electron transferring and ion diffusing rate respectively [18].Jorge Rodríguez-Moreno*et al*., described his work solely on the hybrid nanostructured electrode on ITO/glass substrates wherein we have explained the effect of metal sulfides and the effect of each layer on the fabrication of hybrid nanostructured electrodes on NF. The obtained interesting electrode structure plays a vital role in providing more active sites for electrochemical reactions, short ion and electron diffusion pathways and facilitated ion transport. As a results, a

maximum specific capacitance of 2554.61 and 2040.73 F g^{-1} are measured for ZnONRs@CuS@PEDOT: PSS@MnO_2 and ZnONRs@CuS@PEDOT: PSS at 0.71 A g^{-1}, whereas the pure ZnO and ZnO@CuS displays a specific capacitance of 24.77 and 1709.34 F g^{-1}.

II. EXPERIMENTAL SECTION

2.1 Preparation of nickel foam substrate

$Zn(CH_3COOH)_2.2H_2O$, $Zn(NO_3)_2.6H_2O$, HMT, $C_6H_{12}N_4$, $NiCl_2.6H_2O$, thiourea, 3-MPA , ethylene glycol , copper chloride dehydrate, sulfur were purchased from Aldrich and used without further purification.All the chemicals were used without further purification. Before the deposition of ZnO@CuS@PEDOT:PSS@MnO_2, the nickel foam (approximately 2 cm x 1.5 cm) was cleaned carefully with a concentrated HCl solution (37 wt.%) by sonication for 10 min to remove the surface oxide layer. The foam was then washed sequentially with acetone, ethanol, and deionized water (DI) for 10 min each to ensure that the surface of the nickel foam was well cleaned. After drying with a hair dryer, the well cleaned nickel foam was transferred to a flask.

2.2 Synthesis of ZnO nanorods

ZnO NRs were prepared by a two-step chemical bath deposition method (CBD). The first step was to coat a ZnO seed layer on nickel foam (NF) substrate. The ZnO seed layer was prepared using zinc acetate dihydrate 10 mM [$Zn(CH_3COOH)_2$. $2H_2O$] as a precursor, dissolved in ethanol and stirred for 30 min. then it was annealed at 65 ºC for 5 h in ambient air. The second step was to grow ZnO NRs on the seeded NF using a CBD method. The seeded substrate was suspended upside down in an aqueous solution containing 0.015 M zinc nitrate hexahydrate ($Zn(NO_3)_2.6H_2O$) and hexamethylenetetramine (HMT) ($C_6H_{12}N_4$) at 95 ºC for 15 h to grow ZNO NRs. After being washed with ethanol and DI water for several times, the as-prepared ZnO NRs were annealed at 65 ºC for 5 h.

2.3 Synthesis of CuS nanoparticles

Preparation of CuS, the metal source copper chloride dihydrate (0.1mol) was firstly dissolved in 100 ml of ethyl glycol. The solution were stirred for 20 min under ambient condition followed by addition of 0.1 mol sulfur and stirred for further 10-15 min at 40 ºC and then the solutionwas transferred into a Teflon-lined autoclave heated to 150ºC for 6h. After cooling to ambient temperature, the obtained CuS material were filtered and washed with DI water and ethanol for two to three times. The CuS were dried in vacuum oven at 55 ºC for 4 h. The as prepared materials (CuS) were used to prepare supercapacitor electrodes.

2.4 Fabrication of working electrode

NF with applied ZnO NRs are further used here. CuS powder and a small amount of ethanol were added to produce a homogeneous paste. This paste was then pressed onto ZnO coated NF to produce ZnO@CuSelectrodes, which were vacuum dried for 4 h at 55°C. The industrial use of high performance PEDOT:PSS to work as efficient and conductive platform matrix on ZnO@CuS nanoparticles, the prepared electrodes were dip-coated twice into PEDOT:PSS for 10 min each. The polymer-coated electrodes (ZnO@CuS@PEDOT:PSS) were dried in a vacuum for 12 h at 60 ºC.To coat the ZnONR@CuS@PEDOT:PSSand decorate with MnO_2 nanoparticles, these samples (ZnO@CuS@PEDOT:PSS@MnO_2) have been drop casted using 10mM $KMnO_4$ aqueous solution.The step by step coating procedure for the resultant electrodes is shown in Figure 1. ZnO, ZnO@CuS, ZnO@CuS@PEDOT:PSS, and ZnO@CuS@PEDOT:PSS@MnO_2coated substrates was densely coated and kept nearly opaque and named as Z, ZC, ZCP, and ZCPM, respectively. The weight of the active material was almost 7-10 mg cm^{-2} for all electrodes.In supporting information we have clearly explained about electrochemical measurements, characterization and equations for calculating specific capacitance and energy and power densities.

ISSN 2348 – 8034
Impact Factor- 5.070

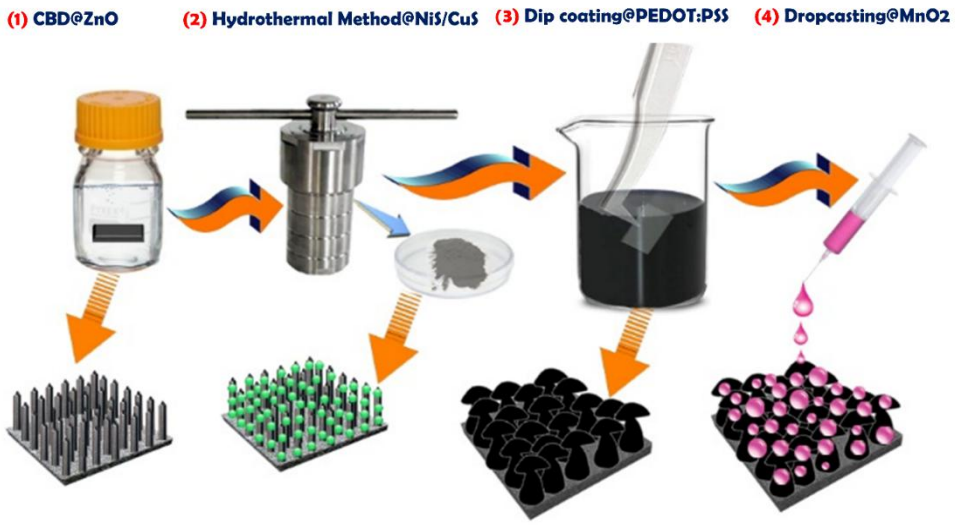

Figure 1. Step by step synthesis procedure of the hybrid nano-structured electrodes.

III. RESULTS AND DISCUSSION

A schematic illumination of the morphological evolution process of the ZnO NRs@CuS@PEDOT:PSS@MnO_2 is represented in Figure 2. The large contact area between the current collector (ZnO nanorods) and active material (CuS) can significantly shorten the electron transportation path length. Next, the decorating active nanomaterial (MnO_2) on ZnO (current collectors)can lead to the escalation in number of electrochemically active sites for the redox reaction that enables rapid diffusion of the cations during the charge discharge process. After that densely arranged ZnONRs@CuS@PEDOT:PSSon the NF substrate offers more electrochemically active sites for nucleation and growth of MnO_2.

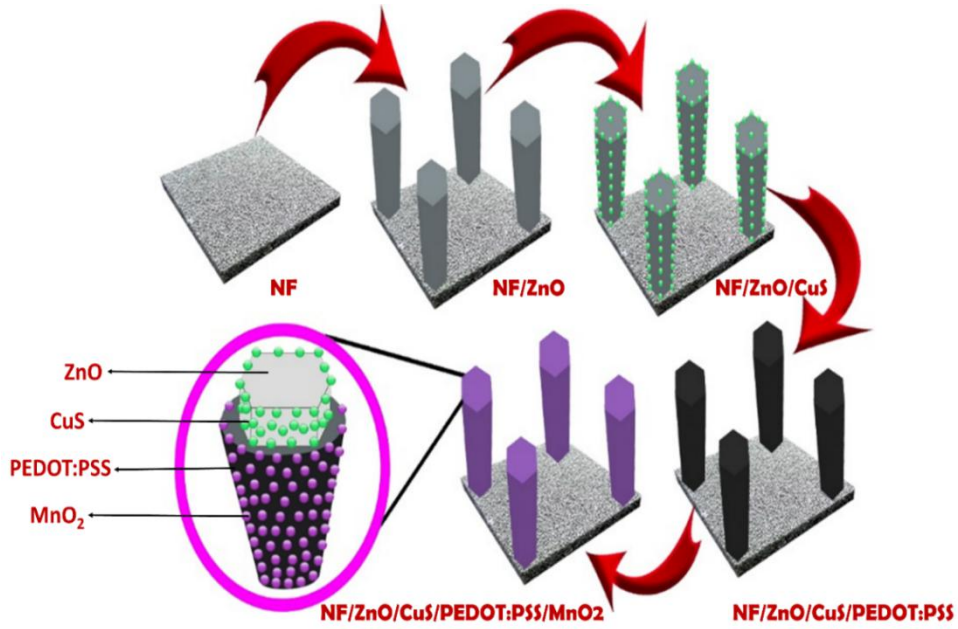

Figure 2. Schematic diagram of fabrication procedure for the designed ZnO/CuS/PEDOT:PSS/MnO_2 nanostructured electrode.

3.1 Surface morphology, and structural characterization of the prepared electrodes

SEM images of Z, ZC, ZCP and ZCPM and their corresponding high magnification images are shown in Figure3. For the deposition of CuS on the Z (ZC), the CuS nanoparticles are uniformly decorated on the surface of the Z. It was found that the deposition of CuS (Figure 3 (b)) did not destroy the morphology of the ZC. The uniform distribution of CuS nanoparticles arose from the growth mechanism and CuS aggregates are formed on the ZnO NRs which increases the number of reactive sites for the reaction [18]. Consequently, the void spaces between the NRs were filled with metal sulfides that formed a network wrapping theZnO NRs. This results in improved electronic conductivity between, yielding more defects and an enhancement of the charge transport process compared to the bare ZnOmaterial.CuSis deposited onto the ZnO NRs for enhance charge transport ability along each single Z and to provide heterogeneous nucleation sites for the growth of the PEDOT:PSS layer [19]. It can be demonstrated that this CuS layer is composed of nano-crystalline aggregates. The SEM images also proposed that during the CuS coating on networks of ZnO NRs and NF, the particle sizes were extremelydecreased in order to enhance the surface area. It is well identified that the nanoparticles on porous structures can facilitate the transport of electrons and secureefficientsurface contact between the active material and the redox electrolyte [20].

When PEDOT:PSS (Figure3(c))conductive polymer shell layer is grown on theZC using dip coating onto the surface of the ZC it ultimately form a core–shell structure.Lastly, in order to grow the MnO_2 nanoparticles, through a redox exchange process, decoration of the ZCP nanostructures by MnO_2 nanoparticles was achieved. The addition of PEDOT:PSS which develops the cohesiveness between MnO_2, and bothPEDOT:PSS and MnO_2 thatcombines well with each other.As shown in Figure3(d), the SEM image of ZCPMnanostructure suggests that a PEDOT layer could be successfully deposited. Furthermore, over the smooth PEDOT layer, the presence of the MnO_2nanoparticles (NPs) can be concluded from the roughness that the ZCPM nanostructure. Nearly all the hybrid core–shell NRs are highly accessible to redox electrolytes for electrochemical energy storage due to the existence of suitable diffusion channels.

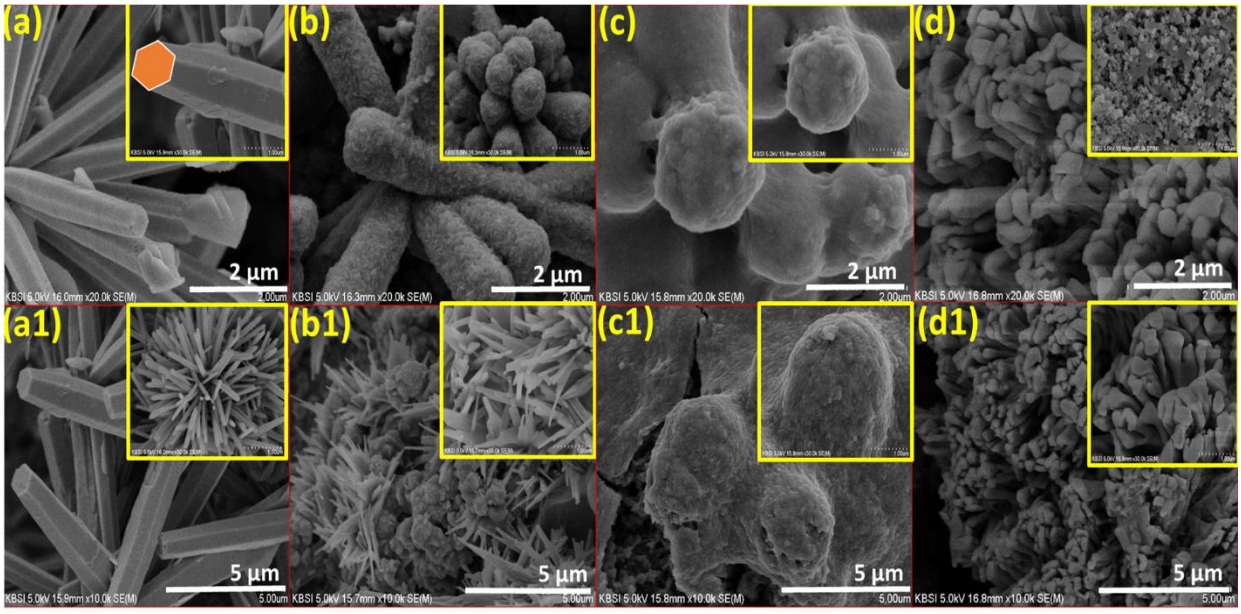

Figure 3. Field emission scanning electron microscopy images of (a) ZnO (b) ZnO/CuS (c) ZnO/CuS/PEDOT:PSS (d) ZnO/CuS/PEDOT:PSS/MnO_2 and their corresponding high magnification images (a1, b1, c1 and d1).

The intrinsic morphology of Z, ZC, ZCP and ZCPM was further investigated by TEM. TEM images (Figure 4 (b)) of CuS on ZnO NRs (ZC) nanostructure discloses that the core shell is formed. The average particle size of ZC is found to be ~1 to 1.5 µm from the TEM images. Moreover, When PEDOT:PSS is coated there were no interlayer gaps between nanoparticles, indicating that the CuS NPs were strongly attached to ZnO NRs. The synergetic

interaction between PEDOT:PSS, CuS and ZnO NRs may help the improvement of the catalytic activity and longer stability for supercapacitor applications. In contrast, TEM images of ZCP (Figure 4 (c)) showed large agglomerated particles, which are consistent with FE-SEManalysis. For comparison, the intrinsic morphology of ZCPM was explained using TEM (Figure 4 (d)), which confirms the deposition of the ZCPM. These outcomedeclares that a uniform-sizedCuS NP with hierarchical core−shell structure, which may increase electron transfer rates.

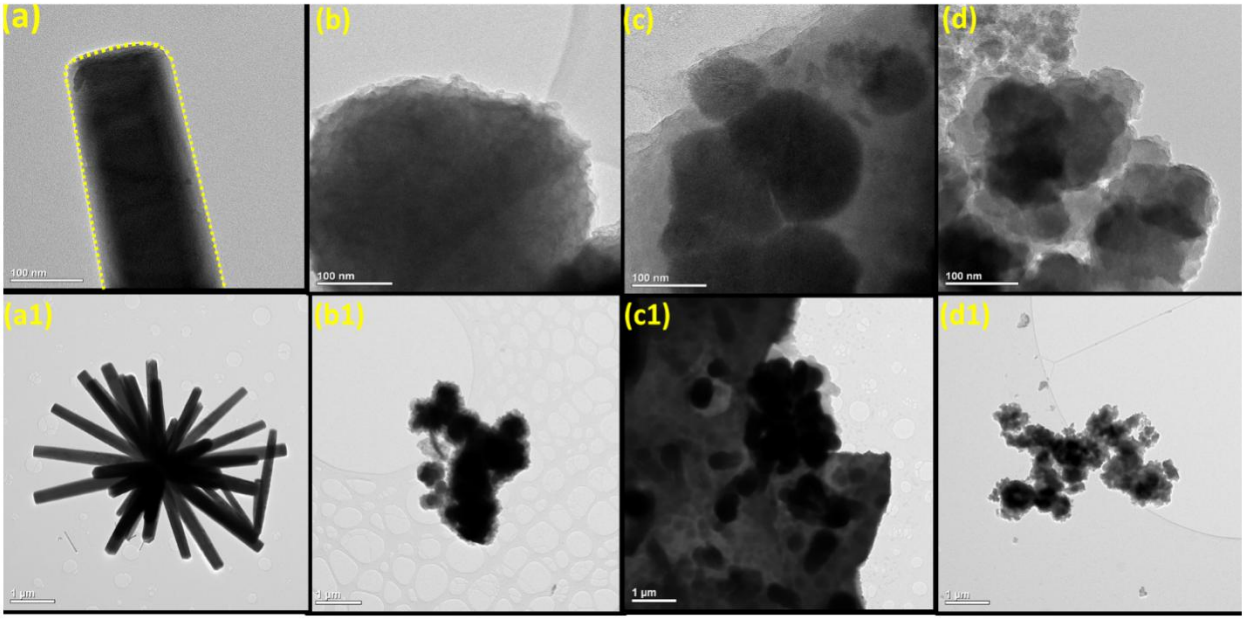

Figure 4. Transmission electron microscopy images of (a) ZnO (b) ZnO/CuS (c) ZnO/CuS/PEDOT:PSS (d) ZnO/CuS/PEDOT:PSS/MnO_2 and their corresponding high magnification images (a1, b1, c1 and d1).

The chemical composition and surface electronic state of the electrodewith certain regularity in distribution is one of the important characteristics which guarantee superior electrochemical property.X-ray photoelectron spectroscopy (XPS)was used to identify all the elements valence states and their specific ratios for the prepared electrodes(Figure 5).The strong resolution Zn 2p spectrum is presented in (Figure 5(a)), of which two strong peaks at 1022.02 and 1045.05 eV can be clearly seen, corresponding to the binding energy of Zn $2p_{3/2}$ and Zn $2p_{1/2}$, respectively, indicating the presence of Zn^{2+} in the ZnO wurtzite structure [21].It is observed that there is an energy separation of 23 eV between the Zn 2p3/2 and Zn 2p1/2 peaks, which is in agreement with an earlier report on ZnO [22].

ISSN 2348 – 8034
Impact Factor- 5.070

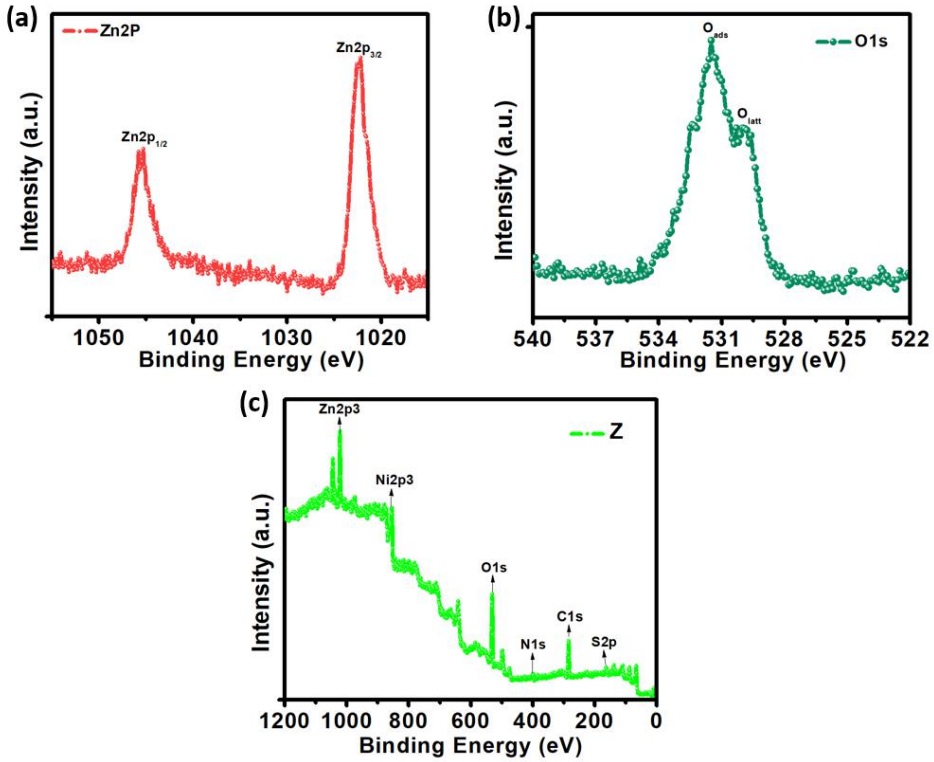

Figure 5. XPS of (a) Zn2p (b) O1s and (c) survey spectrum of ZnO on nickel foam substrate

From the O1s spectrum (Figure 5(b)), it can be seen the spectrum can be fitted to two gauss peaks which one is O_{latt} (530.51 eV) and the other one is O_{ads} (531.77 eV). O_{latt} is defined as oxygen ions in the crystal lattice, while O_{ads} is the absorbed oxygen ions in the oxygen deficient regions.These functional groups are beneficial to capacitive performance because they can contribute to additional pseudo-capacitance and improve the wettability between electrode and electrolyte [23]. The survey spectrum of ZnO is given in Figure 5 (c),ZnOpeaks, which confirms the presence of Zn species in the electrode along with O1s and Cls peaks.

The XPS results shows that the ZC electrode consists of Cu and S elements with ZnO (Figure 6 (a)).Thetwo peaks of Cu2p are obtained at binding energy in the range of 932 to 952 eV relative to the $2p_{1/2}$ and $2p_{3/2}$regions, which shown inFigure 6 (d) [24].Sulfur peaks were also obtained at 162 eV. The absence of a sulfonate peak proposes in elevation of stability when using CuS and a lower reactive rate with atmospheric oxygen. These elements with corresponding binding energies are consistent with previously stated CuS, though the $S2p_{3/2}$ and $S2p_{1/2}$ binding energies are higher than that of the CuS crystal that describes the vigorous bonding between CuS and ZnO [25].The greater bonding between CuS and ZnO NRs can enhance the charge transfer rate and also increase the cycle life of the electrode materials. These results validated that the CuS NPs are well sum up by the ZnO/CuS/PEDOT:PSS and are also successfully fabricated by the current coating techniques. The presence of mammoth numbers of surface functional groups is responsible for preventing agglomeration of CuS in the ZnO/CuS and ZnO/CuS/PEDOT:PSS/MnO_2.The high-resolution Mn 2p spectrum (Figure 6 (f)) shows that $Mn2p_{1/2}$ $Mn2p_{3/2}$ having binding energies at 653.7 eV and 641.9 eV, respectively, with an energy separation of 11.8 eV, are in good agreement with the previous results for MnO_2 [26].EDX analysis was also used to examine the elemental compositions of Z, ZC, ZCP and ZCPM and theresults is shown in Figure S1 in supporting information.

ISSN 2348 – 8034
Impact Factor- 5.070

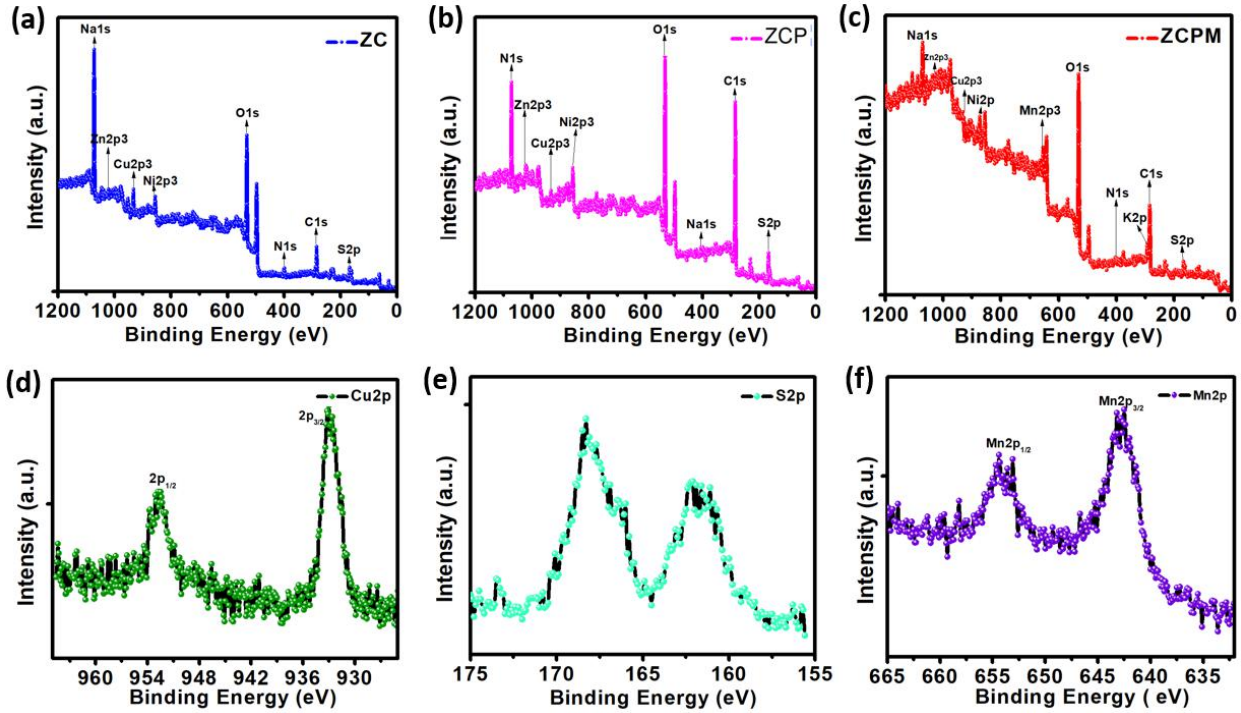

Figure 6. XPS survey spectrum of (a) ZnO/CuS, (b) ZnO/CuS/PEDOT:PSS, (c) ZnO/CuS/PEDOT:PSS/MnO_2 and XPS analysis of (d) Cu2p, (e) S2p of CuS and (f) Mn2p scan

3.2 Electrochemical studies and specific capacitance measurements

To explore the energy storage for the prepared hierarchical supercapacitor electrodes was investigated by characterizing electrochemical studies. Electrochemical measurements were carried out for the Z, ZC, ZCP and ZCPM based electrodes in a three-electrode electrochemical cell with 2 M KOH aqueous solution is used as the electrolyte.Figure 7 (a-d) shows the CV curves of the electrodes recorded at various scan rates in the potential range of -0.1 to 0.7 at different scan rates for Z, ZC, ZCP and ZCPM electrodes. Figure 7 (a-d) displays a pair of redox peaks that indicate the electrochemical performance of electrodes resulting from pseudo-capacitive behaviour. The cathodic peak current increases to a more cathodic direction while increasing the scan rates from 5 to 100 mV/s which could be attributed to the high conductivity of the electrode[18]. The capacitance increases with decrease in the scanning rate and it is evident that this is associated with the adsorption and desorption of ions at available sites. When moving on to higher scan rates, the ions do not get enough time to get into the available sites. Though at lower scan rates the ions diffuse and get adsorbed at available sites with increase in the specific capacity of the material [18].

ISSN 2348 – 8034
Impact Factor- 5.070

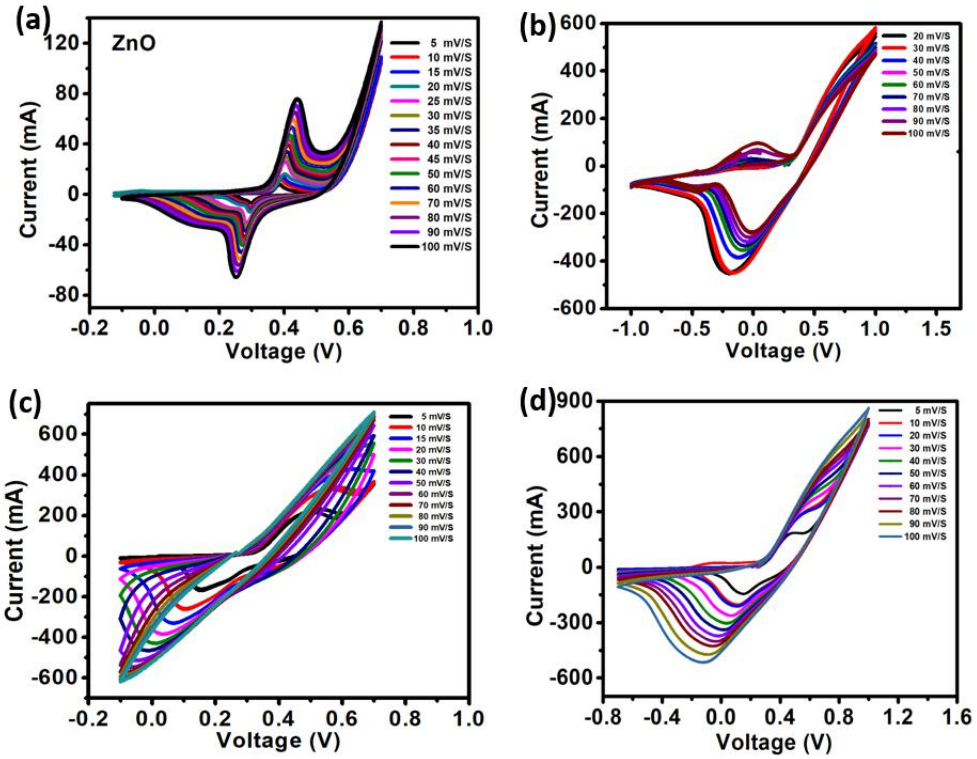

Figure 7. Cyclic voltammetry of (a) ZnO, (b) ZnO/CuS, (c) ZnO/CuS/PEDOT:PSS and (d) ZnO/CuS/PEDOT:PSS/MnO_2 at different scan rates from 5 to 100 mV s^{-1} in 2 M KOH solution.

The CV of electrode Z (Figure 9 (a)) consists of a pair of redox peaks which are observed in the CV curve caused by the redox reactions of ZnO. This redox process is mainly governed by the intercalation and de-intercalation of K^+ from electrolyte into ZnO as shown in equation (1).

$$ZnO + K^+ + e^- \leftrightarrow ZnOK \quad (1)$$

When CuS is coated on ZnO (Figure 7 (b)), there is no doubt that such a structure will have high specific area and can improve the adsorption efficiency of ion, resulting in the strong capacitance of the material [27-28].The ZC electrode showed a larger CV area, which suggests a higher capacitance and the high performance of the ZC electrode was endorsed to the material with a high specific surface area and high porosity, which improves the transport of ions to the active sites of the electrodes. When PEDOT:PSS is added to ZC, there is an enhanced specific current for the composite film which is due to its good synergetic effect between them.This enlarges the contact area between the active materials and electrolytes. ZCP electrode shows higher current when compared with ZC electrode because of its fast electron transfer kinetics of ions on the resultant electrode surface and hence offers more active sites for the nucleation and growth of MnO_2(Figure 7 (c)).

MnO_2 is coated on ZCP (Figure 7 (d)), the polymer supported NR structures enables fast access of ions to the surface on MnO_2.Capacitance of MnO_2comes mainly from pseudo-capacitance ascribed to reversible redox reactions in conjunction with the intercalation/adsorption of protons and/or cations. ZCPM shows highest current in comparison with that of Z, ZC, and ZCP, suggesting that the ZCPM electrode exhibits much better pseudo-capacitive performance and electrochemical reversibility. The detailed oxidation and reduction current values of each sample is given in the supporting information (Table S1).

ISSN 2348 – 8034
Impact Factor- 5.070

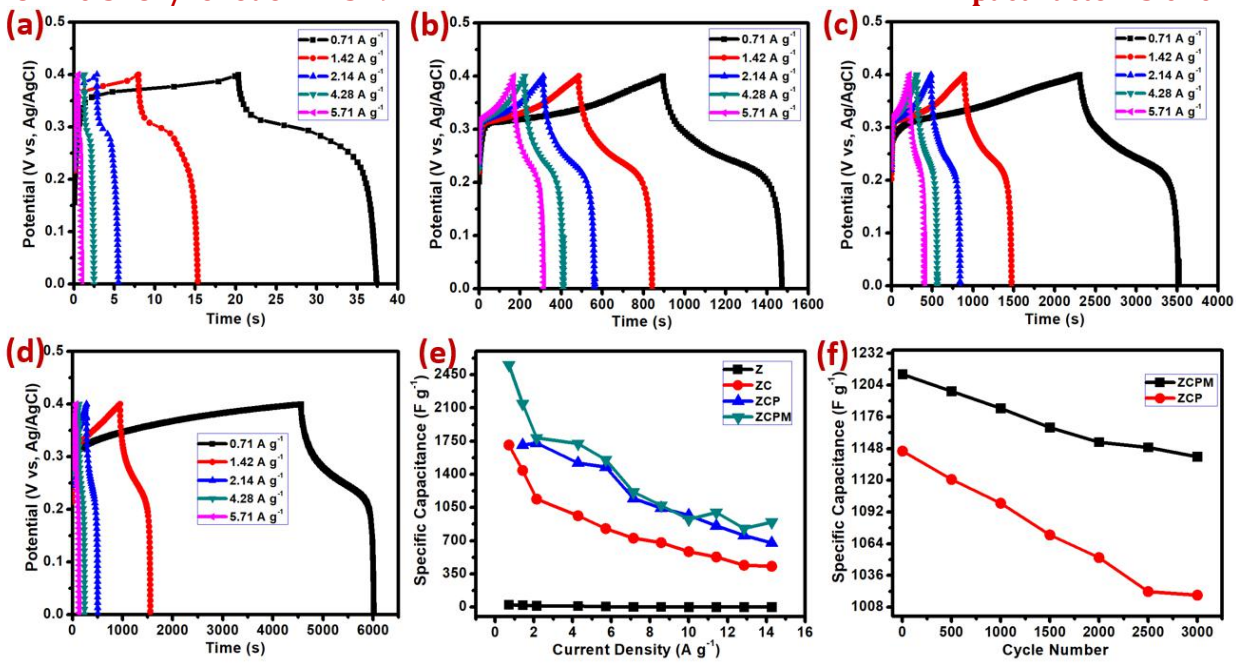

Figure 8. Galvanostatic charge-discharge curves of (a) ZnO, (b) ZnO/CuS, (c) ZnO/CuS/PEDOT:PSS, (d) ZnO/CuS/PEDOT:PSS/MnO_2, and (e) graph showing specific capacitances of ZnO, ZnO/CuS, ZnO/CuS/PEDOT:PSS and ZnO/CuS/PEDOT:PSS/MnO_2 at different current densities. (f) Cyclic stability of ZnO/CuS/PEDOT:PSS/MnO_2 and ZnO/CuS/PEDOT:PSS at current density of 5.71 A g^{-1} for 3000 cycles.

Galvanostatic charge–discharge (GCD) is the most accurate technique for capacitance measurements, hence, GCD measurements were conducted for samples Z, ZC, ZCP and ZCPM (Figure 8 (a-d)) within the potential window of 0−0.4 V at different current densities of 0.71, 1.42, 2.14, 4.28, and 5.71 A g^{-1}. The specific capacitance can be declines with the increase of the current density because of internal resistance drop (IR drop), which is caused by equivalent series resistance, which includes electrolyte, electrode and contact resistance between the electrode and the electrolyte.Discharge profile of theZ, ZC, ZCP and ZCPM electrodes was found to depend on the applied current and similar curve shapes have been attained for various current densities[26].The ZCPM electrode exhibited the longest discharge duration compared to the Z,ZC, and ZCP reflecting the substantially superior performance. These results show that the specific surface area and mesoporous structures with a uniform morphology are crucial factors for obtaining high supercapacitor performance.The detailed specific capacitance values of each electrode is given in the supporting information (Table S2).

Moreover, the specific capacitance of ZCPM were calculated to be 2554.61, 2143.61, 1704.76, 1466.34, 1259.16, 1095.92, 954.28, 840.4, 736.8, 650.91 and 568.14 F g^{-1} at current densities of 0.71, 1.42, 2.14, 4.28, 5.71, 7.14, 8.57, 10.00, 11.42, 12.85, 14.28 A g^{-1},respectively. As the current density increased from 0.71 to 14.28 A g^{-1}, the capacitance of the ZCPM electrode decreased from 722.41 to 470.25 F g-1, which is a relatively high capacitance retention (i.e., 65.09%). The capacitive performance of the ZCPM min electrode was superior to that of the other electrodes due to the higher diffusion and migration of electrolytic ions as well as to the use of the inner active surface area for charge storage at high current densities [29].The excellent electrochemical performances of the core-shell structures (ZCPM) can be attributed to its unique hierarchical structure which can provide more active sites for electrochemical reactions.Comparison of specific capacitance values of different composite electrode materials with previously reported nanostructures using standard three-electrode cell is given in the supporting information (Table S3).

To further investigate the cycling stability, the as-prepared ZCP and ZCPM electrodes were evaluated at a constant charge-discharge current density of 5.71 A g^{-1} for 3000 cycles in KOH solution, as shown in Figure 8 (f). It can be

ISSN 2348 – 8034
Impact Factor- 5.070

clearly seen that the ZCP electrode for the 1st cycle showed a specific capacitance of 1145.82 F g^{-1}, which reducedgradually to 1018.63 F g^{-1} after 3000 cycles, showing 11.1 % loss. On the other hand, the ZCPM electrode, initially for first 500 cycles the capacitance increased from 1095.92 F $g^{-1}$to 1213.61 F g^{-1}. After 500 cycles the capacitance reduced and finally it exhibited only 6% loss of a specific capacitance after more than 3000 cycles, highlighting the good long-term stability of the ZCPM electrode.

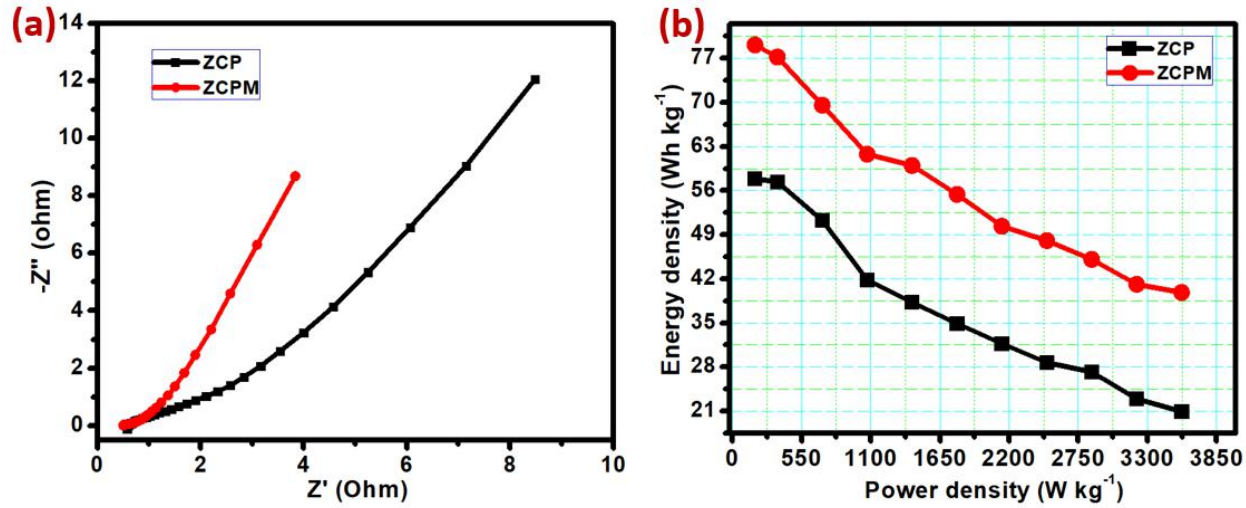

Figure 9.(a) Nyquist plot and (b) Ragone plot of the as prepared ZnO/CuS/PEDOT:PSS and ZnO/CuS/PEDOT:PSS/MnO_2 electrodes.

To discuss the transport characteristics of the charge carries in sample of ZCP and ZCPM electrodes, the electrochemical impendence spectroscopy (EIS) was also accompanied at open circuit potential over the frequency range 100 KHz to 0.1 Hz. Using this EIS spectra, in Figure 9 (a),the Nyquist plots shapes a semicircle at high frequency regions and an inclined line in low frequency. At higher frequencies, the point that intersects with the real axis exhibits an internal resistance (R_S), while the diameter of the semicircle is related to the interfacial charge transfer resistance (R_{ct}) and electrolyte interface. It can be seen that the slope of the straight line for the ZCPM nanocomposite electrode is larger than that of the ZCP electrode, That is to say the ZCPM nanocomposites have a better ions diffusion in the electrode which is seen in Figure 9(a). At high frequencies, the point intersecting with the real axis of the ZCPM nanocomposite electrode is smaller than of the ZCP electrode which means that the conduction of the ZCPM nanocomposites was improved by compositing the active material with good electrical conductivity. The better ion diffusion can be ascribed to the morphology of the ZCPM nanocomposites possessed core-shell structure ZCP as well as larger specific surface area, which are beneficial to the ion diffusion, and the specific capacitance was improved. The overall resistance values of the ZCP and ZCPM based electrodes are the combination of R_s and R_{ct} values, which was found to be lower for ZCPM (1.64 Ω) and higher for ZCP electrode (2.81 Ω).The power density and energy density are two essential parameters to examine the performance of supercapacitors. Figure 9 (b) shows the Ragone plots of ZCP and ZCPM. The ZCPM exhibited a high energy density (79.14 W h Kg^{-1}) and power density (178.57 W kg^{-1}), which were much higher than those of ZCP (57.91 W h Kg^{-1}) at a current density of 0.71 A g^{-1}.

To summarize, a scalable strategy and an approach has been developed to fabricate transparent hierarchical ZCPM hybrid nanoarchitectures with an enhanced electrochemical performance for supercapacitors. The enhanced capacitive behavior is attributed to the unique hierarchical core–shell hybrid nanorod array configuration and the synergistic effects of ZnO NR current collectors and the combined pseudo-capacitive contributions from the PEDOT@NPs MnO_2 shell layer. The metal sulfide nanostructures would provide more active sites to catalyze the reduction of electrolyte and this particles are directly anchored on the surface of the vertically aligned ZnO NRs to ensure higher electrical conductivity and uphold fast charge transport.

ISSN 2348 – 8034
Impact Factor- 5.070

IV. CONCLUSIONS

We reported a facile and cost-effective hydrothermal, chemical bath deposition method along with dip coating to synthesize ZnO@CuS@PEDOT:PSS@MnO_2 (ZCPM) hetero-structures. The resultant electrode (ZCPM) exhibited numerous advantages such as higher deployment rate of electrode in KOH solution, easy penetration of ions into inner region of the electrode, and an enhanced faradic reaction of the electrode surface area with electrolyte compared to other electrodes (Z, ZC and ZCP).The ZCPM electrode shows a high capacitance of 2554.61F g^{-1} at a current density of 0.71 A g^{-1} and good long-term cycling stability of 94 %, which is superior to that of the ZCP electrode. The outstanding performances are profiting from its unique porous structure constructed by interlaced nanoparticles. Our future work will be focused on further improving the cycling stability of remaining electrodes with different metal sulfides. The overall improved electrochemical performance of the ZCPM electrode makes it promising for potential applications in high performance supercapacitor.

V. Acknowledgements

This research was supported by Basic Research Laboratory through the National Research Foundations of Korea funded by the Ministry of Science, ICT and Future Planning (NRF-2015R1A4A1041584). We also thank KBSI for HR-SEM, EDX, XRD and XPS measurements.

Notes

The authors declare no competing financial interest. The samples were analyzed by Transmission electron microscopy (TEM, JEM-2011) and scanning electron microscope (SEM, Hitachi S-4200) with a 4k x 4k CCD camera (Ultra Scan 400SP, Gatan corp.) at the Busan KBSI, South Korea

REFERENCES

1. *Selvakumar M, Krishna BD, Manish AA, Prahladh IS,Sravani G, 2010 Nano ZnO-activated carbon composite electrodes for supercapacitors.Physica B: Condensed Matter,405,2286-2289.*
2. *Li X, Wang Z, Qiu Y, Pan Q,Hu PA, 2015 3D graphene/ZnO nanorods composite networks as supercapacitor electrodes.Journal of Alloys and Compounds620,31-37.*
3. *Wang J,Gao Z,Li Z,Wang B,Yan Y,Liu Q,Mann T,Zhang M,Jiang Z, 2011 Green synthesis of graphene nanosheets/ZnO composites and electrochemical properties.J. Solid State Chem., 184,1421-1427.*
4. *Rao SS,Punnoose D,Kim SK,Kim HJ, 2015Low-cost solution processed nano millet like structure CoS_2 film superior to Pt as counter electrode for quantum dot sensitized solar cells.Electron. Mater. Lett.,11,485-493.*
5. *Consonni V, Rey G,Bonaime J, Karst N,Doisneau B, Roussel H,Renet S,Bellet D, 2011Low temperature LO-phonon dynamics of MgZnO nanoalloys.Appl. Phys. Lett., 98, 111906-3.*
6. *SunYK,Chen Z,Noh HJ,Lee DJ,Jung HG,Ren Y,Wang S,Yoon CS,Myung ST,Amine K, 2012 Nanostructured high-energy cathode materials for advanced lithium batteries.Nature Materials, 11, 942-947.*
7. *Li LQ,Yang HB,Yang J,Zhang LP,Miao JM,Zhang YF,Sun CC,Huang W,Dong XC,Liu B, 2016Hierarchical carbon@Ni_3S_2@MoS_2 double core–shell nanorods for high-performance supercapacitors.J. Mater. Chem. A,4,1319-1325.*
8. *Rao SS,Durga IK,Kundakarla N,Punnoose D, Gopi CVVM, Reddy AE,Jagadeesh M,Kim HJ, 2017A hydrothermal reaction combined with a post anion-exchange reaction of hierarchically nanostructured $NiCo_2S_4$ for high-performance QDSSCs and supercapacitors.New J. Chem., 41, 10037-10047.*
9. *Kalanur SS,Chae SY,Joo OS, 2013 Transparent $Cu_{1.8}S$ and CuS thin films on FTO as efficient counter electrode for quantum dot solar cells.Electrochimica Acta103,91-95.*
10. *Sagade AA,Sharma R, Copper sulphide (Cu_xS) as an ammonia gas sensor working at room temperature. 2008Sens. Actuator B-Chem, 133,135-143.*
11. *Luo M,Liu Y, Hu J, Li J, Liu J,Richards RM,2012 General strategy for one-pot synthesis of metal sulfide hollow spheres with enhanced photocatalytic activity,Appl. Catal. B Environ. 125,180-188.*
12. *Wang J, Chew SY, Wexler D, Wang GX, Ng SH, Zhong S,Liu HK, 2007 Nanostructured nickel sulfide synthesized via a polyol route as a cathode material for the rechargeable lithium battery.Electrochem. Commun., 9,1877-1880.*

13. Zhang Y, Tian J, Li H, Wang L,Qin X,Asiri A, Al-Youbi A,Sun X, 2012Biomolecule-Assisted, Environmentally Friendly, One-Pot Synthesis of CuS/Reduced Graphene Oxide Nanocomposites with Enhanced Photocatalytic Performance.Langmuir, 28,12893-12900.
14. Mane R,Lokhande C, 2000 Chemical deposition method for metal chalcogenide thin films,Mater. Chem. Phys., 65,1-31.
15. Manickam MS,Avijit B, David M, Rob J, Carlos F, 2016 Correlation among physical and electrochemical behavior of nanostructured electrolytic manganese dioxide from leach liquor and synthetic for aqueous asymmetric capacitor. Phys. Chem. Chem. Phys.,18, 4711-4720.
16. Subramanian V, Zhu HW,Vajtai R,Ajayan PM,Wei BQ, 2005Hydrothermal Synthesis and Pseudocapacitance Properties of MnO_2Nanostructures.J. Phys. Chem. B, 109,20207-20214.
17. Hou Y, Cheng YW, Hobson T,Liu J, 2010Design and Synthesis of Hierarchical MnO_2 Nanospheres/Carbon Nanotubes/Conducting Polymer Ternary Composite for High Performance Electrochemical Electrodes.Nano Lett., 10,2727-2733.
18. Rodrı´guez-Moreno J, Navarrete-Astorga E,Dalchiele EA,Schrebler R, Ramos-Barrado JR,Martın F, 2014Vertically aligned ZnO@CuS@PEDOTcore@shell nanorod arrays decorated with MnO_2 nanoparticles for a high-performance and semi-transparent supercapacitor electrode.Chem. Commun., 50,5652-5655.
19. Wang ZH,Geng DY,Zhang YJ,Zhang ZD, 2010CuS:Ni flowerlike morphologies synthesized by the solvothermal route.Mater. Chem. Phys. 122,241–245.
20. Wu Z,Li L,Yan J,Zhang X, 2017Materials Design and System Construction for Conventional and New-Concept Supercapacitors.Adv. Sci. 4,1600382.
21. Rao SS,Punnoose D,Tulasivarma CHV,Kumar CHSSP, Gopi CVVM, Kim SK, Kim HJ, 2015 A strategy to enhance the efficiency of dye-sensitized solar cells by the highly efficient TiO_2/ZnS photoanode.Dalton Trans., 44,2447-2455.
22. Wu C,Cai J, Zhu Y, Zhang K, 2016Nanoforest of hierarchical core/shell CuO@$NiCo_2O_4$nanowire heterostructure arrays on nickel foam for high-performance supercapacitors.RSC Adv., 6, 63905-63914.
23. Rao SS,Punnoose D, Bae JH, Durga IK, Varma CVT, Naresh B,Subramanian A, Raman V,Kim HJ,Preparation and electrochemical performances of NiS with PEDOT:PSSchrysanthemum petal like nanostructure for high performance supercapacitors.Electrochimica Acta254, 269-279.
24. Ludwig J, An L,Pattengale B, Kong X,Xi P,HuangJ, 2015Ultrafast Hole Trapping and Relaxation Dynamics in p-Type CuSNanodisks. Phys. Chem. Lett. 6,2671-2675.
25. Rao SS, Durga IK, Varma CVT,Punnoose D, Cheol LJ, Kim HJ, 2015The synthesis and characterization of lead sulfide with cube-like structure as a counter electrode in the presence of urea using a hydrothermal method.New J. Chem., 39, 7379-7388.
26. Qiang L, Jianhua L, Jianhua Z,Anindarupa C,Yiqing C, Lei Z, 2011 Synthesis and electrochemical performance of multi-walled carbon nanotube/polyaniline/MnO_2 ternary coaxial nanostructures for supercapacitors.Journal of Power Sources196, 565-572.
27. Ramya R, Manickam MS, 2016 A biopolymer gel-decorated cobalt molybdate nanowafer: effective graft polymer cross-linked with an organic acid for better energy storage, New J. Chem., 40, 2863-2877.
28. Manickam M, Maryam JB, Robert TJ, 2017 Rescaling metal molybdate nanostructures with biopolymer for energy storage having high capacitance with robust cycle stability.Dalton Trans., 46, 3588-3600.
29. Li T,Zuo Y, Lei X, Li N,Liu J,HanH, 2016Regulating the oxidation degree of nickel foam: a smart strategy to controllably synthesize active Ni_3S_2nanorod/nanowire arrays for high-performance supercapacitors. J. Mater. Chem. A, 4,8029-8040.